

## Supporting Information

### Atomic Scale Quantum Anomalous Hall Effect in Monolayer

### Graphene/MnBi<sub>2</sub>Te<sub>4</sub> Heterostructure

Yueh-Ting Yao<sup>1</sup>, Su-Yang Xu<sup>2\*</sup>, Tay-Rong Chang<sup>1,3,4\*</sup>

<sup>1</sup>Department of Physics, National Cheng Kung University, Tainan 70101, Taiwan.

<sup>2</sup>Department of Chemistry and Chemical Biology, Harvard University, Cambridge, MA 02138, USA.

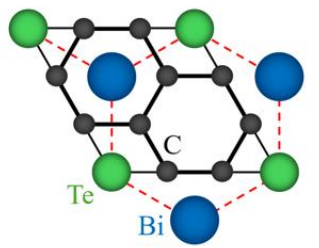
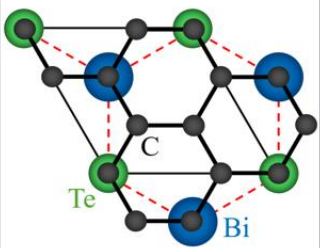
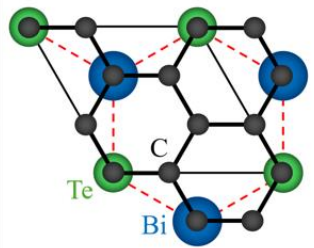
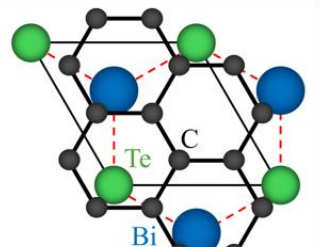
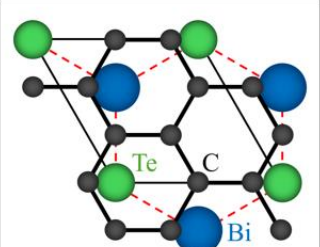
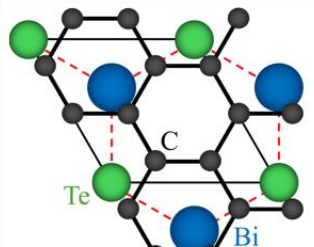
<sup>3</sup>Center for Quantum Frontiers of Research and Technology (QFort), Tainan 701, Taiwan.

<sup>4</sup>Physics Division, National Center for Theoretical Sciences, Taipei 10617, Taiwan.

\*Corresponding Authors: [suyangxu@fas.harvard.edu](mailto:suyangxu@fas.harvard.edu), [u32trc00@phys.ncku.edu.tw](mailto:u32trc00@phys.ncku.edu.tw)

## S1: Stability of Different Stacking Configurations

To validate the stability across various stacking arrangements between graphene and  $\text{MnBi}_2\text{Te}_4$ , we conducted total energy calculations employing DFT, as detailed in Table S1. Table S1 delineates six stacking configurations of graphene/ $\text{MnBi}_2\text{Te}_4$ : one hollow site, two top sites, and three bridge sites. We designate the hollow site as the reference point for total energy, aligning with the stacking configuration depicted in Fig. 1 in the main text. Our findings indicate that alternative stacking configurations exhibit higher total energy compared to the hollow site, thereby reinforcing the stability of the configurations illustrated in Fig. 1.

Type	Hollow Site	Top Site - 1	Top Site - 2
Structure			
$\Delta E$	0 (eV/per cell)	2.88 (eV/per cell)	2.88 (eV/per cell)
Type	Bridge Site - 1	Bridge Site - 2	Bridge Site - 3
Structure			
$\Delta E$	0.02 (eV/per cell)	0.02 (eV/per cell)	0.02 (eV/per cell)

**Table S1.** The total energy values corresponding to various stacking configurations. To enhance clarity, only the topmost three layers of the structure are depicted, comprising graphene (black), one Te layer (green), and one Bi layer (blue).

## **S2: Magnetic Ground State of Graphene/MnBi<sub>2</sub>Te<sub>4</sub>**

In order to validate the magnetic ground state, we have conducted total energy calculations for various magnetic structures using DFT, as outlined in Table S2. The crystal structure of MnBi<sub>2</sub>Te<sub>4</sub> belongs to space group  $R\bar{3}m$  (No. 166), which possesses  $C_3$  rotational symmetry, allowing for the examination of three types of ferromagnetic structures (one out-of-plane and two in-plane) and six types of antiferromagnetic structures (taking into consideration a 2x2 supercell), as elaborated in Table S2. Our findings reveal that the ferromagnetic structure with an out-of-plane spin configuration (FM<sub>out</sub>) exhibits the lowest total energy, thereby indicating the magnetic ground state. It is noteworthy that the magnetic anisotropy energy is relatively small, suggesting that the in-plane spin configuration may be easily achieved by applying an external magnetic field. In this study, we introduce the graphene/MnBi<sub>2</sub>Te<sub>4</sub> heterostructure with an out-of-plane ferromagnetic ground state (FM<sub>out</sub>) as the Chern insulating phase QAH1 with a Chern number of  $C = 1$ . The exploration of identifying topological phase transitions within the alternative magnetic structures represents an intriguing avenue for future investigation.

Type	FM <sub>out</sub>	FM <sub>in,1</sub>	FM <sub>in,2</sub>
Magnetic Structure			
$\Delta E$	0 (eV/per cell)	1.11 (meV/per cell)	1.72 (meV/per cell)
Type	AFM <sub>out,1</sub>	AFM <sub>out,2</sub>	AFM <sub>in,1</sub>
Magnetic Structure			
$\Delta E$	8.14 (meV/per cell)	8.09 (meV/per cell)	8.73 (meV/per cell)
Type	AFM <sub>in,2</sub>	AFM <sub>in,3</sub>	AFM <sub>in,4</sub>
Magnetic Structure			
$\Delta E$	8.66 (meV/per cell)	8.68 (meV/per cell)	9.35 (meV/per cell)

**Table S2.** The total energy of different magnetic configurations. The red sphere represents the Mn atoms of MnBi<sub>2</sub>Te<sub>4</sub>, and the black arrow indicates the magnetic moments.

### S3: Zeeman exchange field of $\text{MnBi}_2\text{Te}_4$ influences the evolution of graphene band structure.

Figure S1 illustrates a schematic diagram elucidating how the Zeeman exchange field of  $\text{MnBi}_2\text{Te}_4$  influences the evolution of graphene band structure. Initially, in the absence of the Zeeman exchange field, graphene manifests a Quantum Spin Hall (QSH2) phase, as depicted in Fig. 2 of the main text, attributed to intrinsic spin-orbit coupling (SOC) and Kekulé distortion. Upon activating the Zeeman exchange field, the band structure of graphene undergoes spin splitting. Once the field strength surpasses a certain threshold, the topmost valence band and the bottommost conduction band in the graphene spin band experience band inversion, leading to the emergence of a topologically nontrivial gap induced by Rashba SOC ( $\lambda_{R2}$ ), thereby achieving the Quantum Anomalous Hall (QAH1) phase. The inset of new Fig. 4(a) illustrate the congruence in the band structure between DFT and effective Hamiltonian model, with both importantly sharing the same Chern number  $C = 1$ .

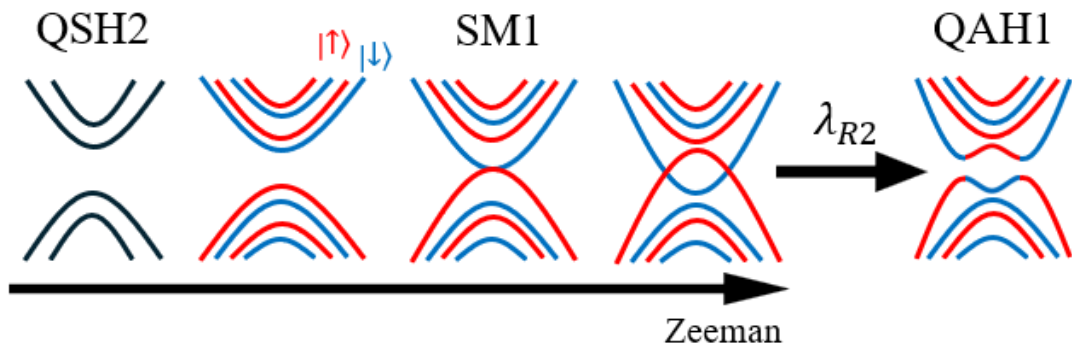


**Figure S1.** A schematic diagram presents the evolution of graphene band structure from QSH2 to QAH1 as the Zeeman exchange field increases.